

# Effect of Magnetostriction on the Core Loss, Noise, and Vibration of Fluxgate Sensor Composed of Amorphous Materials

Chang-Hung Hsu<sup>1</sup>, Chun-Yao Lee<sup>2</sup>, Yeong-Hwa Chang<sup>3</sup>, Faa-Jeng Lin<sup>4</sup>, Chao-Ming Fu<sup>5</sup>, and Jau-Grace Lin<sup>6</sup>

<sup>1</sup>Division of Electrical Engineering, Fortune Electric Company Ltd., Tao-Yuan 320, Taiwan

<sup>2</sup>Department of Electrical Engineering, Chung Yuan Christian University, Tao-Yuan 320, Taiwan

<sup>3</sup>Department of Electrical Engineering, Chang Gung University, Tao-Yuan 333, Taiwan

<sup>4</sup>Department of Electrical Engineering, National Central University, Tao-Yuan 320, Taiwan

<sup>5</sup>Department of Physics, National Taiwan University, Tai-Pei 10617, Taiwan

<sup>6</sup>Center for Condensed Matter Sciences, National Taiwan University, Tai-Pei 10617, Taiwan

This paper presents a new multistructure fluxgate magnetic sensor composed of Metglas® Fe-based amorphous HB1 material. The core thickness of the fabricated structure is 0.0254 mm × 30 pieces, and its width is 5 mm. The magnetic loss of the fluxgate core is simulated through finite element analysis. The fluxgate sensor is experimentally analyzed over a frequency range 0.5–3 kHz. The sensor performance exploits the advantages of the multistructure core-shaped magnetic material as well as the second-harmonic operation mechanism. Excellent flux responses are detected for the triangular core sensor, which has different operating frequencies for magnetostriction variation, harmonic response, total harmonic distortion, noise level, sensor vibration, and sensitivity. The influence of magnetostriction, magnetic loss, and permeability in multiangled cores for different frequencies is analyzed. Our multistructure fluxgate sensor is suitable for various applications including power transformer and inverter for interior magnetic core fault detection, owing to its thin-film configuration, high sensitivity, high resolution, and low magnetic loss.

**Index Terms**—Amorphous core, fluxgate sensor, magnetostriction, sensitivity, vibration.

## I. INTRODUCTION

RECENTLY, there have been many studies investigating magnetic field sensing. Magnetic field measurements are an essential function for numerous applications [1], [2]. Measurements of DC power or slowly varying magnetic fields are significantly more challenging than measurements of AC magnetic fields, which are more straightforward. A number of different techniques and sensors have been developed to detect magnetic fields [3]. The magnetometer device, which has been shown to be a two-axis miniature fluxgate sensor, can be used to obtain two-directional magnetic field measurements.

One of the most sensitive magnetic sensors is the fluxgate sensor, which has a high sensitivity in both its measuring range and resolution [4]. Fluxgate sensors can also be used as orientation sensors for virtual reality applications or as ferromagnetic object detectors. Multicore fluxgate sensing elements are fabricated from micro-wire arrays with Ni-Fe/Cu wires [5]. Sensors with different numbers of wires and different structures have been proposed. The longitudinal hysteresis loops show that the magnetic anisotropy of the arrays changes for the different structures [6]. Much of the focus has been on reducing the size of the fluxgates, making devices lightweight and low cost, and integrating them into the supporting electronic circuitry [7], [8]. Increasing the sensitivity of Ni/Co is important. However, Ni/Co is an expensive material and is therefore not suitable for wide industrial use in electrical device applications.

This paper proposes multistructure fluxgate sensors composed of Fe-based amorphous HB1 material. The presence of

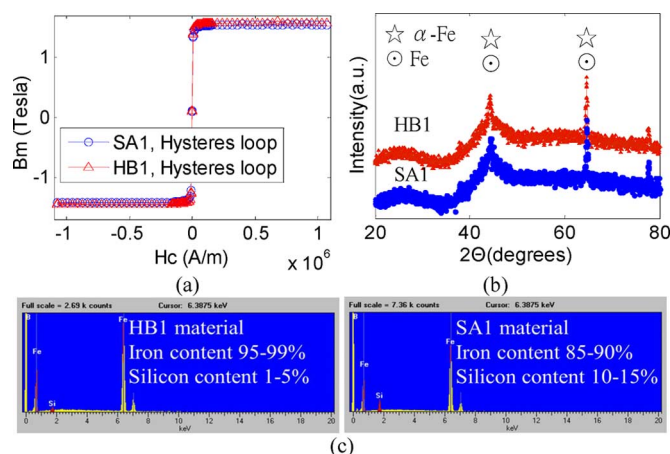


Fig. 1. Measured results of the magnetic properties for amorphous materials HB1 and SA1: (a) VSM, (b) XRD, and (c) EDS.

different core-structures is effective in overcoming the drawbacks of previous sensor devices. This paper is organized as follows. In Section II, the simulation, design, and fabrication of the multistructure fluxgate sensor are described. In Section III, the experimental results are discussed. Our conclusions are given in Section IV.

## II. THEORY, DESIGN, AND MAGNETIC PROPERTIES

### A. Amorphous Core Magnetic Property Analysis

Different soft materials of the amorphous core, including HB1 and SA1 with thicknesses of 0.762 mm and widths of 0.5 mm, were analyzed in this study. The amorphous core was annealed at 325 °C (for HB1) and 350 °C (for SA1), and then soaked for 1.5 h. Magnetic properties were measured by using X-ray diffraction (XRD) and a vibrating sample magnetometer (VSM) as shown in Fig. 1(a) and (b). Besides, energy dispersing spectroscopy (EDS) is used to detect material compositions, as shown in Fig. 1(c).

Manuscript received November 05, 2012; revised January 22, 2013; accepted February 12, 2013. Date of current version July 15, 2013. Corresponding author: C.-H. Hsu (e-mail: chshiu@fortune.com.tw).

Color versions of one or more of the figures in this paper are available online at <http://ieeexplore.ieee.org>.

Digital Object Identifier 10.1109/TMAG.2013.2248702

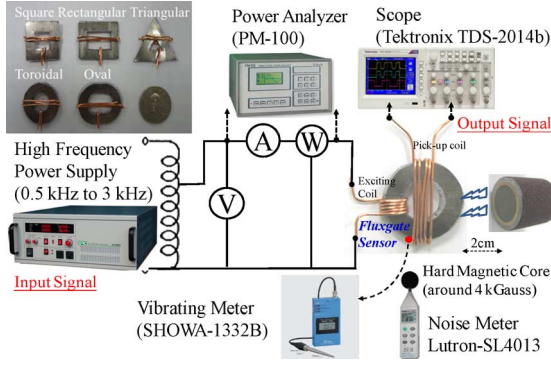


Fig. 2. Schematic diagram showing the experimental system used to measure the fluxgate sensors.

### B. Correlation of Magnetic Loss, Vibration, and Noise Level in a Thin-Film Fluxgate Core

This paper presents the high-permeability characteristics and saturation magnetic induction at approximately 1.64 T of amorphous HB1 material. The experimental setup is shown in Fig. 2; it includes a power meter (PM-100), a vibration meter (SHOWA-1332B), a noise meter (Lutron SL-4013), a high-frequency power supply (IDRC CF-1000), and an oscilloscope (TDS-2014b). The magnetic induction of the core  $B$  was generated by a wired coil and is equal to the curl of the magnetic vector potential  $A$ . The electromagnetic forces for a fluxgate core are defined as

$$B = \nabla \times A \quad (1)$$

$$\nabla \times \frac{1}{\mu} (\nabla \times \vec{A}) = \vec{J}_S - \rho \frac{\partial \vec{A}}{\partial t} \quad (2)$$

where  $\mu$  is the magnetic permeability (H/m),  $\vec{A}$  represents the magnetic vector potential,  $\vec{J}_S$  is the current density (A/m), and  $\rho$  is the conductivity (S/m). In this case, the magnetic flux density distribution at operating frequencies of 500 Hz and 3000 Hz is chosen to analyze sensor core magnetic property using the finite element analysis (FEA), as shown in Fig. 3.

It is indicated that the magnetic flux line passing through a part of the different core corner and core leg exhibits different magnetic property. This implies that the increasing core loss is probably induced by magnetostriction variation [9], as shown in Fig. 3. In recent work by some of the authors of the present paper [10], it has been noted that the core vibration intensity  $\alpha_{\text{core}}$  is proportional to the magnetostriction force, such that  $\alpha_{\text{core}} \propto B_m \propto \varepsilon_s$ , as is well known. This means that  $\alpha_{\text{core}}$  is also proportional to  $\varepsilon_s$ . The noise level  $N_c$  of the magnetic response is such that  $N_c \propto W_t \propto C_L \propto B_m$ , where  $C_L$  (m) is the core length and  $W_t$  (kg) is the core weight. The noise level can arise from the magnetostriction vibration at frequencies of  $2f$ . The acceleration due to magnetostriction vibrations is proportional to the force  $\varepsilon_s$  and in turns of  $N_c$ .

### C. Fluxgate Sensor Design

The fluxgate sensor devices were based on thin-film fluxgate sensors of Metglas® amorphous HB1 magnetic material. The

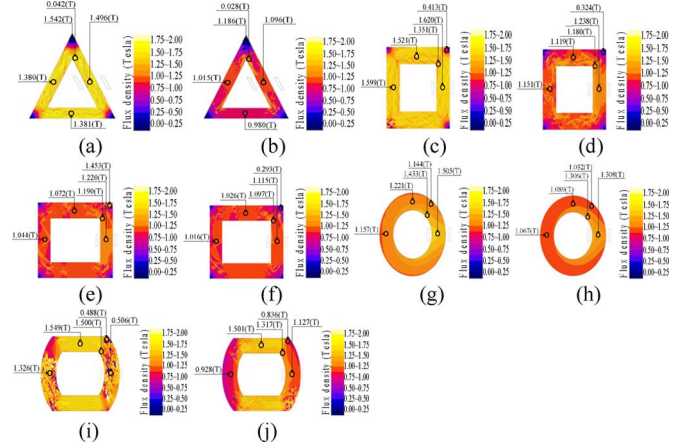


Fig. 3. FEA simulation results of different fluxgate sensors with amorphous material: (a) Triangular core type under 3000 Hz, (b) triangular core type under 500 Hz, (c) square core type under 3000 Hz, (d) square core type under 500 Hz, (e) rectangular core type under 3000 Hz, (f) rectangular core type under 500 Hz, (g) toroidal core type under 3000 Hz, (h) toroidal core type under 500 Hz, (i) oval core type under 3000 Hz, and (j) oval core type under 500 Hz.

thickness of the core was  $0.0254 \text{ mm} \times 30$  pieces, and its width was 5 mm. Single phase sine waves of various frequencies were applied to the excitation coils to drive the core through its B—H curve. The amplitude of the excitation current was adjusted so that the applied magnetic induction was operated at around 1.39 T over the frequency range of 0.5 to 3 kHz. The direction in which the sensing coil faced determined the directionality of the external magnetic field detection. The output signal shows the magnetic flux of the hard external magnetic material  $B_{\text{ext}} \cong 4 \text{ kG}$  that flows through the face area of the sensing coils. It has previously been shown that the Fourier analysis of the induced voltage in the coil for a fluxgate sensor excited by an AC magnetic field with a triangular waveform gives rise to a second harmonic voltage  $V_{2f}$  [11] such that

$$V_{2f} = \frac{8NA\mu_r B_m f}{\pi} \sin \frac{\pi \Delta B}{B_m} \sin \frac{\pi B_{\text{ext}}}{B_m} \quad (3)$$

where  $N$  is the number of turns in the pick-up coil,  $A$  is the cross-sectional area of the core,  $\mu_r$  is the effective relative permeability of the core material,  $B_m$  is the maximum magnetic induction generated by the excitation current, and  $\Delta B = 2B_s/\mu_r$ , where  $B_s$  is the saturation magnetic induction. From (3), the magnetic sensitivity of the fluxgate sensor  $S_B$  can be found such that

$$S_B [V/T] = dV_{2f}/dB_{\text{ext}} = 8NA\mu_r f. \quad (4)$$

Equation (4) clearly shows the linear dependence of the fluxgate sensor magnetic sensitivity on various parameters, particularly the effective relative permeability  $\mu_r$ . An AC signal was applied to the excitation coils. The fluxgate response to an external magnetic field  $B_{\text{ext}}$  was supported by the hard magnetic core, around a magnetic field of 4 kGauss to be achieved. Oscilloscope records and measurements of  $V_{2f}$  were made as a function of  $B_{\text{ext}}$ . The sensitivity  $S_B = (dV_{2f}/dB_{\text{ext}})$  was determined from numerical calculations.

TABLE I  
COMPARISONS OF MEASUREMENT AND SIMULATION ON FLUXGATE SENSOR  
WITH AMORPHOUS MATERIALS

Category	Operating Frequency	Core loss (Watt/g)	
		Measured results	FEA results
Triangular core	500 Hz	0.815	0.782
	3000 Hz	1.069	1.049
Square core	500 Hz	0.987	0.951
	3000 Hz	1.28	1.22
Rectangular core	500 Hz	0.949	0.921
	3000 Hz	1.29	1.257
Toroidal core	500 Hz	1.116	1.098
	3000 Hz	2.568	2.466
Oval core	500 Hz	1.059	1.024
	3000 Hz	1.56	1.491

### III. EXPERIMENTAL RESULTS AND DISCUSSION

#### A. Magnetic Response of the Fluxgate Sensor

According to the Maxwell's equation as referred to (1) and (2), a comparison of both the FEA results and measured results for the fluxgate sensor in core loss at different frequencies were compared, as shown in Table I.

For different core-structured measurement results, the time-dependence of the pick-up voltage for the fluxgate sensors is shown in Fig. 4, where the driving frequency was between 0.5 kHz to 3 kHz. Equations (3) and (4) can be used to explain the behavior observed in Fig. 4 and to understand the operation of the different fluxgate sensors. It can be measured by the pick-up coil, since the components of the generated flux pass through sensing coil. When an external magnetic field is applied ( $B_{\text{ext}} \cong 4 \text{ kGauss}$ ) in fixing 2 cm distance and an external magnetic flux will appear in the pick-up coil. This adds to the excitation flux and the total time-dependent magnetic field for the ferromagnetic material, where the two sections will no longer be equal in magnitude. This result can be explained by considering the induced voltage  $V_{i,1} = (d\phi/dt)$  in the excitation coil when an external flux line is applied in the second excitation coil in the presence of  $B_{\text{ext}} = 4 \text{ kGauss}$ . The magnetic flux variation  $d\phi/dt$  also represents the time variation of the magnetic flux in the ferromagnetic material within the pick-up coil. The voltage signal  $V_{2f}$  is observed to increase with  $B_{\text{ext}}$ . For triangular sensors, the sensitivity is better than another counterpart of sensor device. A different core-structure in magnetic property of hysteresis loop can be observed as in Fig. 5, where the triangular-type amorphous core can obtain a higher magnetic induction.

#### B. Effect of Magnetostriction, Noise Levels, and Vibrations on Variable Fluxgate Sensors

For the magnetostriction, vibration, and noise level of the fluxgate sensor device, the experimental results show that a lower core vibration between low and high frequency can be obtained for different sensors, as shown in Fig. 6. It is indicated that a long-leg physical shape is suitable at higher frequencies. However, long-leg sensors are not suitable for reducing the excitation current, because the core processes higher magnetic resistance. Fig. 7 shows the plots for the harmonic response and

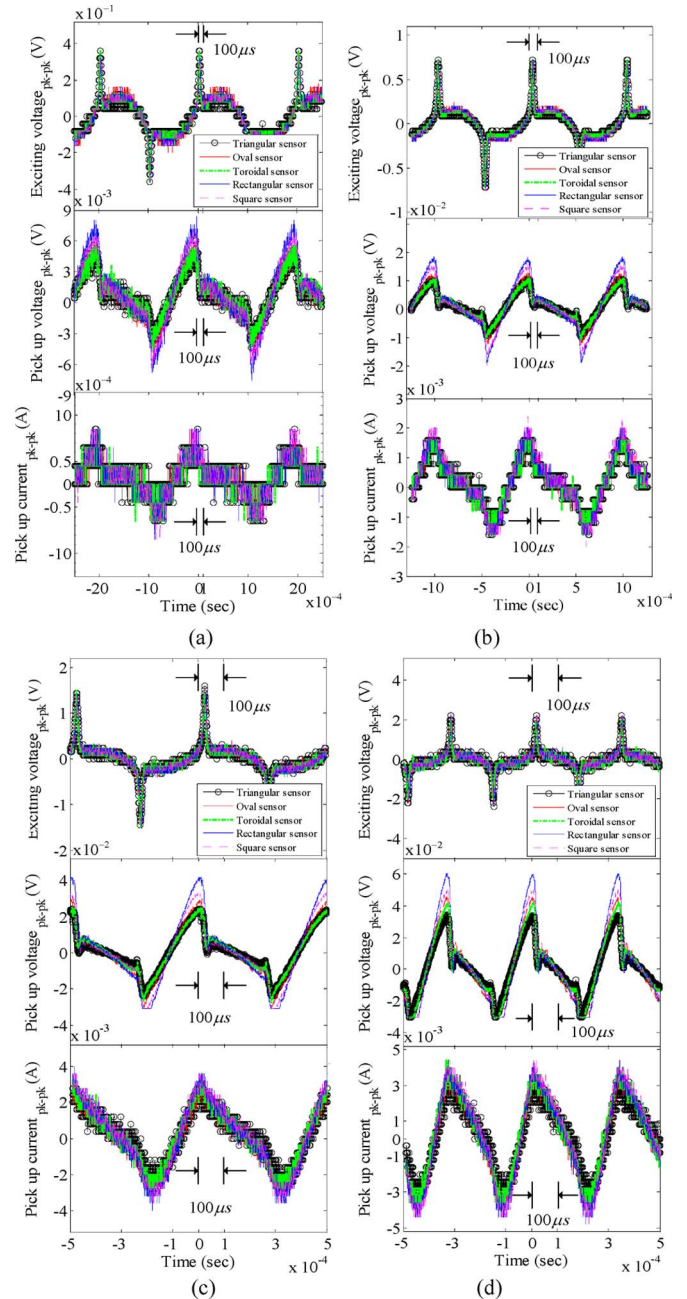


Fig. 4. Measured results of the magnetism property of an amorphous fluxgate sensor under an excitation voltage, pick-up coil voltage, and pick-up coil current during 0.5–3 kHz: (a) 500 Hz, (b) 1000 Hz, (c) 2000 Hz, and (d) 3000 Hz.

the total harmonic distortion (THD) for the fluxgate sensors. One origin for the induced electric pollution of the harmonic may be the different magnetostriction variation of core structures. The opposite behavior is seen in the sensor sensitivity and noise level. It also shows the second harmonic voltage  $V_{2f}$  of the pick-up coil for the fluxgate sensors as a function of  $B_{\text{ext}}$  for various excitation currents  $I_e$  at frequencies  $f$  ranging from 0.5 to 3 kHz, where  $B_{\text{ext}}$  was applied perpendicular to the pick-up coils. Both triangular and rectangular sensors have a lower core vibration and noise level. In fact, a long leg and straight core result in a steady magnetic flux passing through the core, which improves the magnetic sensor properties.

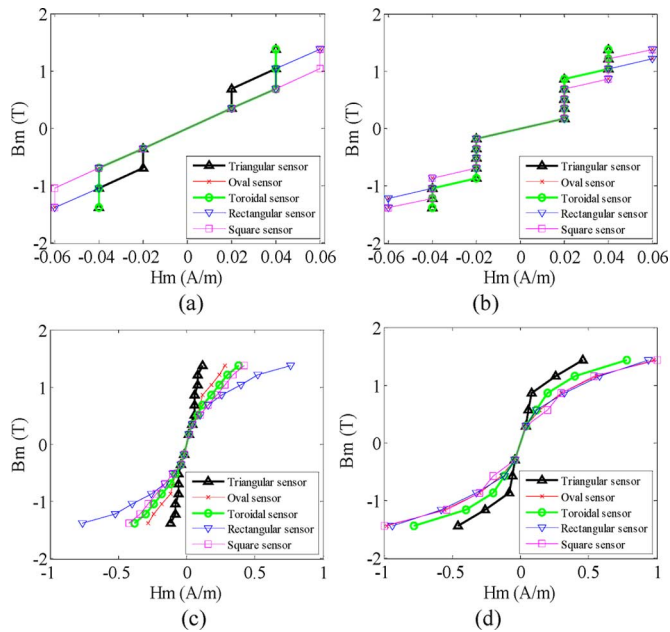


Fig. 5. Measured results of the hysteresis loop of the fluxgate sensor over the range 0.5–3 kHz: (a) 500 Hz response, (b) 1000 Hz response, (c) 2000 Hz response, and (d) 3000 Hz response.

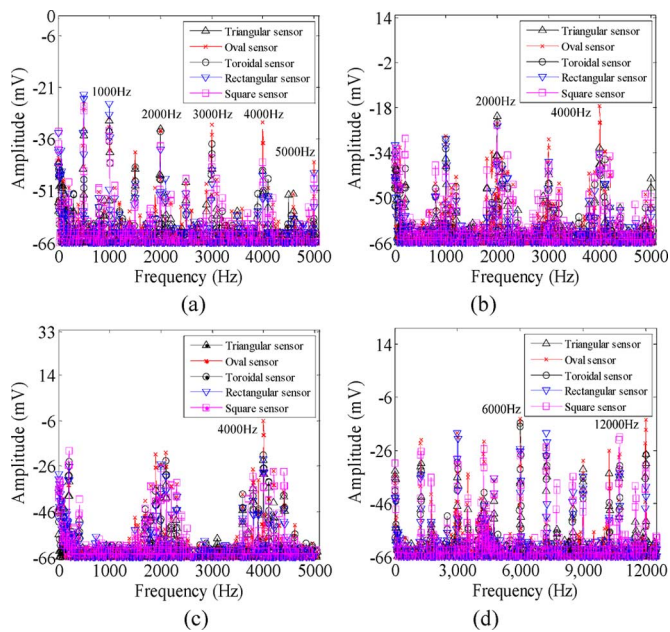


Fig. 6. Fast Fourier transformation (FFT) of different core vibrations at different frequencies: (a) operating at 500 Hz, (b) operating at 1000 Hz, (c) operating at 2000 Hz, and (d) operating at 3000 Hz.

#### IV. CONCLUSION

This research examined thin-film fluxgate sensors composed amorphous HB1 after continuous annealing for 1.5 h. Multi-structure fluxgate sensors possess magnetic properties such as magnetostriction, core loss, sensitivity, harmonic response, THD, noise level, and core vibration. It is indicated that changes in sensitivity, harmonic response, THD, and vibration at different frequencies arise because of the influence of the core-shape and the permeability and magnetic induction of the

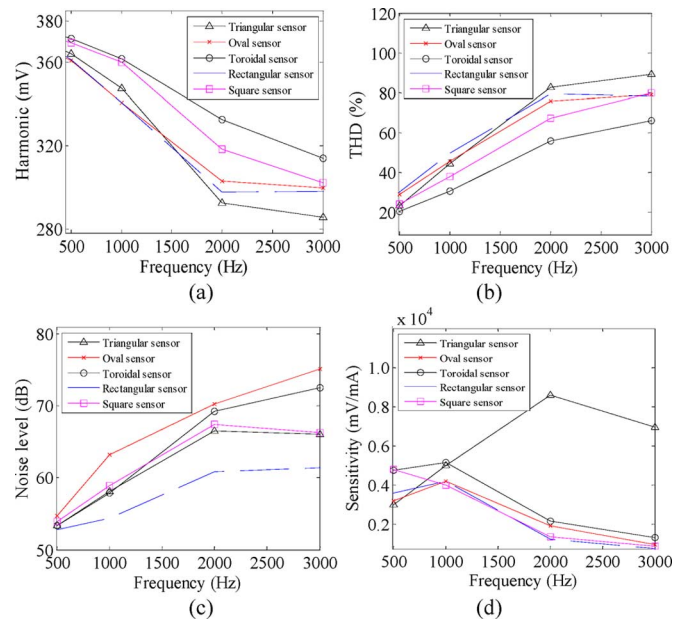


Fig. 7. Results of measurements of a fluxgate sensor made of amorphous materials: (a) harmonic response, (b) total harmonic distortion, (c) noise level, and (d) sensitivity.

sensor. The resulting magnetic properties of the fluxgate sensor, which are a result of its shape, make the sensors suitable for high-frequency applications.

#### REFERENCES

- [1] A. Baschiroto *et al.*, “Development and comparative analysis of fluxgate magnetic sensor structures in PCB technology,” *IEEE Trans. Magn.*, vol. 42, no. 6, pp. 1670–1680, Jun. 2006.
- [2] X. G. Yang, B. Zhang, Y. H. Wang, Z. G. Zhao, and W. L. Yan, “The optimization of dual-core closed-loop fluxgate technology in precision current sensor,” *J. Appl. Phys.*, vol. 111, no. 11, pp. 07E722-1–07E722-3, 2012.
- [3] P. Frydrych, R. Szewczyk, J. Salach, and K. Trzcinka, “Two-axis, miniature fluxgate sensors,” *IEEE Trans. Magn.*, vol. 48, no. 4, pp. 1485–1488, Apr. 2012.
- [4] S. Tumanski, “Induction coil sensors—A review,” *Meas. Sci. Technol.*, vol. 18, no. 3, pp. R31–R46, 2007.
- [5] F. Jie *et al.*, “Study of the noise in multicore orthogonal fluxgate sensors based on Ni-Fe/Cu composite microwave arrays,” *IEEE Trans. Magn.*, vol. 45, no. 10, pp. 4451–4454, Oct. 2009.
- [6] M. R. Kirchoff, A. Jordan, and S. Büttgenbach, “Influence of seed layer systems and their premagnetization by low temperature annealing on electrodeposited Ni-Fe fluxgate cores,” *IEEE Trans. Magn.*, vol. 47, no. 1, pp. 161–169, Jan. 2011.
- [7] Y. Kim, B. Yoon, Y. H. Kim, C. S. Yang, and K. H. Shin, “Wide range orthogonal fluxgate sensor fabricated with cylinder-shaped ferrite core,” *IEEE Trans. Magn.*, vol. 47, no. 10, pp. 3744–3747, Oct. 2011.
- [8] T. M. Liakopoulos and C. H. Ahn, “A micro-fluxgate magnetic sensor using micromachined planar solenoid coils,” *Sensors Actuators A: Phys.*, vol. 77, no. 1, pp. 66–72, 1999.
- [9] C. H. Hsu *et al.*, “Effects of magnetomechanical vibrations and bending stresses on three-phase three-leg transformers with amorphous cores,” *J. Appl. Phys.*, vol. 111, no. 7, pp. 07E730-1–07E730-3, 2012.
- [10] Y.-H. Chang, C. H. Hsu, H. L. Chu, and C. P. Tseng, “Magnetomechanical vibrations of three-phase three-leg transformer with different amorphous-cored structures,” *IEEE Trans. Magn.*, vol. 47, no. 10, pp. 2780–2783, Oct. 2011.
- [11] O. Dezuari, E. Belloy, S. E. Gilbert, and M. A. M. Gijs, “New hybrid technology for planar fluxgate sensor fabrication,” *IEEE Trans. Magn.*, vol. 35, no. 4, pp. 2111–2117, Aug. 1999.